

Interaction of Hydrogen with Pt-Silicalite

P. Mériaudeau,¹ A. Thangaraj, C. Naccache, and S. Narayanan*

*Institut de Recherches sur la Catalyse, CNRS, 2 av. Albert Einstein, 69626 Villeurbanne Cédex, France; and *Indian Institute of Chemical Technology (IICT), Hyderabad, India*

Received December 7, 1993; revised February 18, 1994

Very small Pt particles (6–8 Å) located inside pores of silicalite have been prepared. These Pt particles exhibit peculiar behaviour towards H₂ chemisorption (H/Pt = 2). Infrared studies indicate the presence of hydrogen species vibrating at 3200 cm⁻¹ which are tentatively correlated to extra hydrogen chemisorbed. © 1994

Academic Press, Inc.

INTRODUCTION

The characterisation of zeolite entrapped metal clusters by H₂ or CO chemisorption generally provides a way to evaluate the number of exposed atoms. However, as indicated by Sachtler and Zhang (1), when the metal particles are quite small the ratio of chemisorbed hydrogen to metal (H/M) or chemisorbed CO to metal (CO/M) fails to provide reliable information on metal dispersion. Indeed some reports indicate that a H/Pt stoichiometry higher than 1 can be obtained (2).

The origin of such high H/Pt values is not clear and could be due either to a change in the chemisorptive properties of Pt with the nature of the support and/or to a migration of hydrogen from the metal to the support. Such a hydrogen migration is well documented for noble metals like Pt, Pd, and Rh (3) and it has been shown that the spill-over hydrogen can be at the origin of an increase of the hydrogenation activity (3, 4).

Recently we have prepared ultradispersed Pt particles in silicalite supports exhibiting interesting properties for *n*-octane cyclisation (5). Since these solids showed unusual adsorption properties towards hydrogen, the interaction of hydrogen with ultra dispersed Pt has been investigated by volumetric measurements and IR spectroscopy. These two techniques will provide quantitative and qualitative data concerning H₂ adsorption. In addition, TEM was utilized to estimate the particle size diameters.

¹ To whom correspondence should be addressed.

EXPERIMENTAL

Silicalite support was prepared according to the following method: 36 g of tetraethylorthosilicate (TEOSi) was mixed with 15 g of tetrapropylammonium hydroxide (TPAOH, 20% in water, Aldrich) and 70 g of distilled water. Then the clear solution was crystallized at 170°C for one day at autogeneous pressure. The support so obtained was washed with distilled water and dried in air at 100°C overnight. The template was removed under N₂ stream at 500°C followed by calcination from RT to 500°C under a flow of O₂ in order to remove the coke which could have been formed during the decomposition of the template. Pt(NH₃)₄(OH)₂ was introduced in the zeolite using the "exchange impregnation" technique: the required amount of Pt was added to 100 cm³ of water and the silicalite was slowly added under stirring, *T* being maintained at 70°C overnight. Then the water was removed using a vaporotator pump and the sample was dried at 100°C in air for 4 h. With such a procedure all the platinum of the solution was deposited onto the support. Pt loadings of 0.5, 2, 4 wt% were obtained. Pt (0.5 wt%) Na ZSM-5 was prepared according to the same procedure, Na ZSM-5 being from a commercial source (P.Q., USA).

Hydrogen, oxygen adsorption studies. Samples were activated using the following procedure:

—decomposition of Pt(NH₃)₄²⁺ by flowing O₂ (2 l h⁻¹), *T* being raised from RT to 300°C (ramping 0.2°C/min);

—flushing with N₂ (15 min);

—reduction under H₂ (2 l h⁻¹) from 300°C to 500°C (ramping 1°C/min)

—flushing with N₂ at 500°C (15 min) and cooling down to RT; the as-reduced samples were contacted with air at RT (for characterization by TEM, the samples have to be transferred into the microscope).

Volumetric measurements. Before volumetric measurements, samples were reduced *in situ* in static condi-

tions (with $p_{\text{H}_2} = 50$ kPa) in presence of a liquid N_2 trap, the reduction temperature being fixed at 500°C . The samples were then outgassed under vacuum ($p = 10^{-2}$ Pa) for 30 min before cooling down to RT and used for adsorption experiments. A first isotherm (with H_2 or O_2) was obtained using a classical volumetric apparatus equipped with a Texas gauge to measure the pressure. Having obtained the first isotherm, the sample was outgassed for 10 min at RT ($p = 10^{-1}$ Pa) and a second isotherm was performed. The H/Pt (or O/Pt) values have been calculated by extrapolating both isotherms at zero pressure and considering that the volume of irreversibly adsorbed gas is equal to the difference between the first and the second isotherms. For some samples, titration of adsorbed H_2 by O_2 hydrogen titration (HT) or of adsorbed O_2 by H_2 oxygen titration (OT) was done using the same procedure.

TEM. Studies were performed on samples used for volumetric measurements; a JEOL electron microscope (Jeol 2010) was utilized for this purpose.

IR studies. Samples were pressed into small wafers (15 to 20 mg) which were placed in an infrared cell allowing

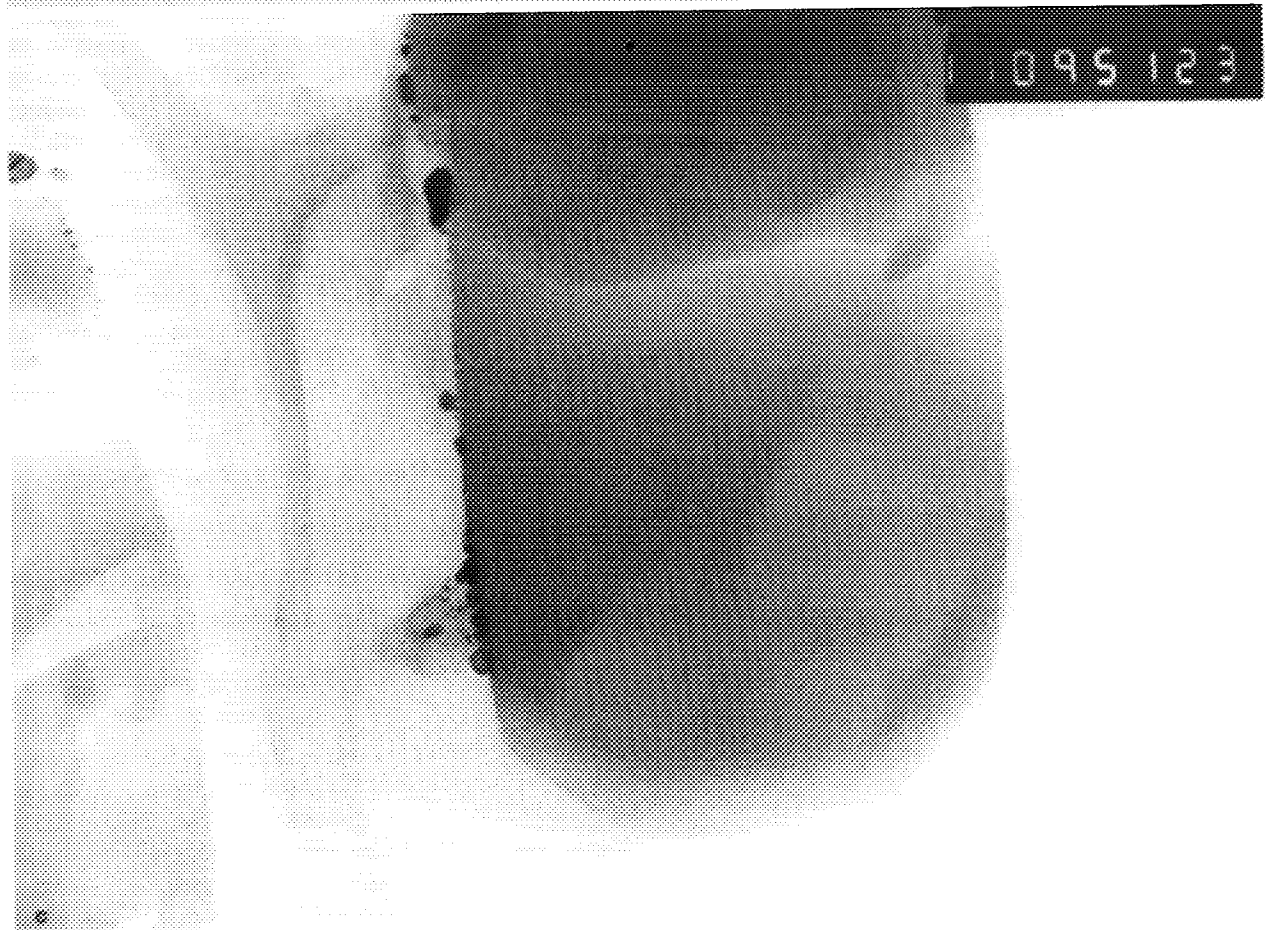
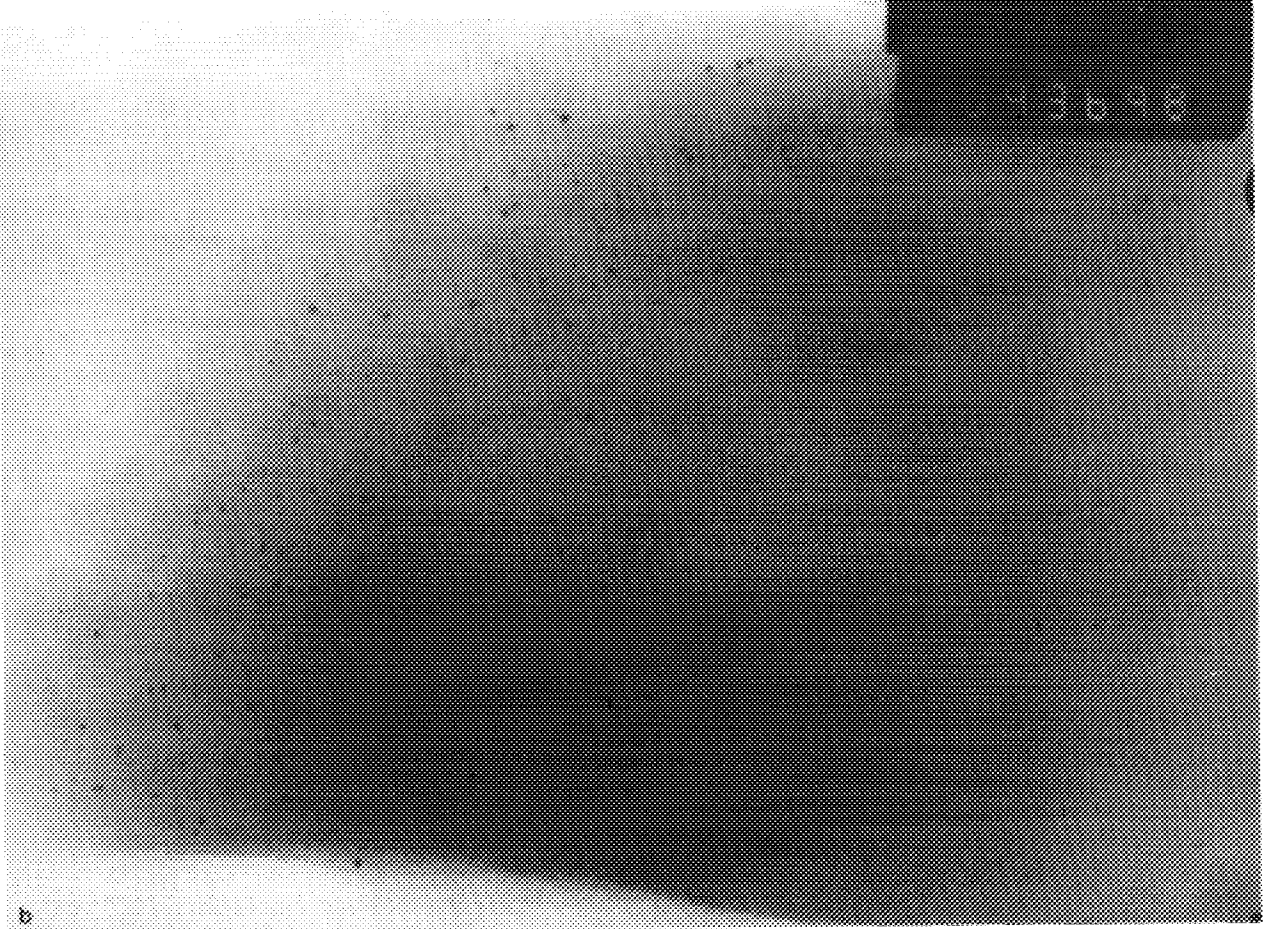
thermal treatments. As for volumetric measurements, samples were re-treated *in situ*. IR spectra were registered at RT using a FTIR Bruker spectrometer (Bruker IFS 48). H_2 , D_2 , and CO , were introduced in the IR cell using a classical glass apparatus.

RESULTS AND DISCUSSION

Transmission electron microscopy studies (TEM). Typical TEM micrographs of the 0.5 wt% Pt-silicalite and 0.5 wt% Pt-NaZSM-5 are given in Figs. 1a and 1b. The sizes of metal particles derived from these micrographs indicated an average particle diameter of 0.6–0.8 nm for Pt-silicalite and 1.2 to 1.5 nm for Pt-NaZSM-5. When the Pt content of the Pt-silicalite catalyst was increased to 2 wt%, the average particle diameter was identical to the 0.5 wt% Pt-silicalite sample (TEM micrographs of 2 wt% Pt sample are not given here). For a higher Pt loading (4 wt% Pt-silicalite), the particle size distribution observed (Fig. 1c) is different: some particles, apparently located within the pore structure have a size less than 1 nm while those located on the external surface



FIG. 1. (a) Micrographs of 0.5 wt% Pt-silicalite (0.7 nm = 1.5 nm). (b) Micrographs of 0.5 wt% Pt-Na ZSM-5 (0.7 nm = 3 nm). (c) Micrographs of 4 wt% Pt-silicalite (0.7 nm = 3 nm).



of the grain have a diameter larger than 1 nm. From these data, two conclusions can be drawn:

- for a low Pt loading (0.5 wt%) Pt particles were much smaller on silicalite support than on NaZSM-5 support;
- on silicalite, up to 2 wt% Pt, the Pt particles are less than 0.8 nm.

VOLUMETRIC MEASUREMENTS

(1) Hydrogen Chemisorption

In Table 1 are reported the hydrogen uptake values obtained on different Pt samples and the atomic ratio H/Pt. As expected from the TEM results, at the same Pt content, the Pt–silicalite solid adsorbed a larger amount of hydrogen than Pt–NaZSM-5 sample. In addition table 1 shows that the increase of Pt content in Pt–silicalite samples decreased the H/Pt ratio, again in agreement with TEM showing that the average particle size increased with the metal content. The most interesting and unexpected result was that the atomic ratio H/Pt obtained on 0.5 and 2 wt% Pt–silicalite samples exceeded the generally accepted value of 1 for H/Pt surfaces. Very small Pt clusters embedded in silicalite adsorbed more than one hydrogen atom per Pt surface atom. In order to have a better knowledge about the behaviour towards hydrogen of these small Pt clusters in silicalite, the titration of adsorbed hydrogen with oxygen (HT), the oxygen adsorption (OA) and the oxygen titration with hydrogen (OT) have been measured.

(2) Oxygen Adsorption, Oxygen Titration, and Hydrogen Titration

The results obtained on 0.5 wt% Pt–silicalite are listed in Table 2 together with the results related to (OT) and (HT). It is clear that oxygen adsorption (O/Pt = 1.05) results are in agreement with the literature. Assuming the

TABLE 1

Hydrogen Chemisorption on Pt Samples

Samples	Pt loading wt%	Hydrogen ($\mu\text{mol catalyst}^{-1}$)	H/Pt
Pt Na ZSM-5	0.5	11.5	0.90
Pt–silicalite	0.5	25.4	1.98
	2	63.8	1.25
	4	38	0.37
Pt–silicalite ^a poisoned with CO	2	4.4	0.08

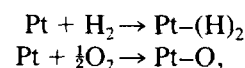
^a Before H₂ chemisorption, sample was reduced under H₂ at 500°C, evacuated at 500°C, cooled down to RT, contacted with CO ($p = 0.5$ kPa) evacuated (10^{-2} Pa) for 15 min and then H₂ chemisorption was performed.

TABLE 2

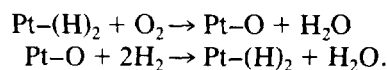
Hydrogen Adsorption (HA), Hydrogen Titration (HT), Oxygen Adsorption (OA), and Oxygen Titration (OT) on 0.5 wt% Pt–Silicalite.

Gas adsorption	Quantity of gas adsorbed ($\mu\text{mol g catalyst}^{-1}$)	H/Pt or O/Pt
Hydrogen (HA)	25.4	1.98
Oxygen (HT)	28	
Oxygen (OA)	13.4	1.05
Hydrogen (OT)	52.5	

following stoichiometry for H₂ and O₂,



one obtains for the hydrogen and oxygen titrations:



From these equations one should obtain HT/HA = 1 and OT/OA = 4. The experimental values derived from Table 2 are respectively 1.1 and 3.9, which is close to the expected theoretical values. Table 1 has also shown that H/Pt ratio decreased from 1.98 to 1.25 with the increase of the Pt loading from 0.5 wt% to 2 wt%. Despite the fact that it is not possible from TEM results to observe a significant increase in particle size between 0.5 wt% Pt and 2 wt% Pt samples, it can be expected that when Pt loading is increased, particle size is also increased; thus it could be suggested that for 2 wt% Pt silicate part of the Pt clusters formed are still adsorbing hydrogen with a H/Pt = 2 (as for 0.5 wt% Pt sample), the other part of Pt clusters (slightly larger) adsorbing hydrogen with the expected stoichiometry H/Pt = 1.

INFRARED INVESTIGATIONS

(1) Infrared Study of H₂ and Exchange with D₂

All the spectra have been obtained in the following way:

- registration of a blank spectrum (after reduction and evacuation), spectrum 1;
- registration of the spectrum after adsorption of a given gas (H₂, CO, etc.), spectrum 2.

Spectra represented on the different figures are the difference between spectrum 2 and spectrum 1. So generally some oscillations are appearing in the 2000–1800 cm⁻¹ range which is the range of framework vibrations; these oscillations could be due either to imperfect subtraction or to change in the lattice vibrations due to the presence

of adsorbed gases on Pt particles. These oscillations are not depending on the nature of the gas adsorbed (H_2 or D_2) and will not be considered in the discussion.

FTIR spectrum of 2 wt% Pt-silicalite having chemisorbed H_2 is represented on Fig. 2a: a broad IR vibration centered at 3200 cm^{-1} together with a less intense vibration at 2030 cm^{-1} were observed. Deuterium adsorption on the bare surface indicated that both the vibrations are shifted to lower wavenumbers (2393 cm^{-1} and 1479 cm^{-1}) (Fig. 2b). A spectrum identical to that represented on Fig. 2b is observed if having chemisorbed H_2 (Fig. 2a) and removed the gas phase at RT for 5 min, D_2 (1 kPa) is contacted the sample. From these results it can be concluded that both the vibrations are due to hydrogen species and that hydrogen is rapidly exchanged with deuterium at room temperature. Same behaviour was obtained with the 0.5 wt% Pt-silicalite sample. It has also to be mentioned that no IR vibration is observed at 1630 cm^{-1} and by consequence the formation of water is unlikely since in such a case, two vibrations (3600 cm^{-1} and 1630 cm^{-1}) are expected. It has to be pointed out that no IR vibration was observed of the silicalite support (free of Pt) when contacted with H_2 ; similarly, no IR vibration was observed when 0.5 wt% Pt-Na-ZSM-5 was contacted with H_2 .

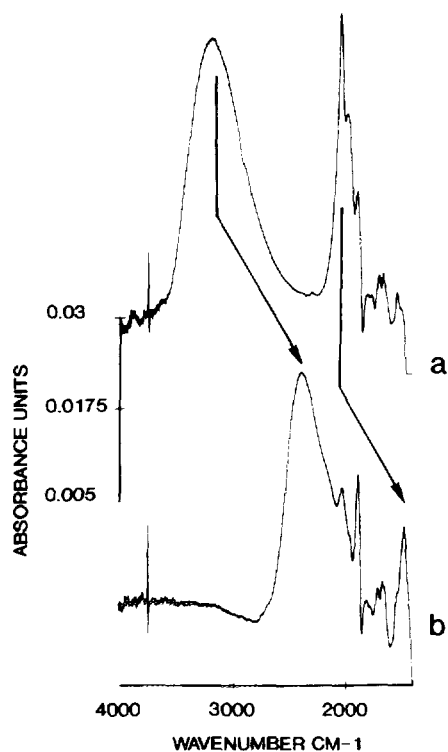


FIG. 2. Infrared spectra of hydrogen adsorbed on 2 wt% Pt-silicalite. See remark (IR investigations). (a) In presence of H_2 ($p_{H_2} = 1\text{ kPa}$). (b) In presence of D_2 ($p_{D_2} = 1\text{ kPa}$).

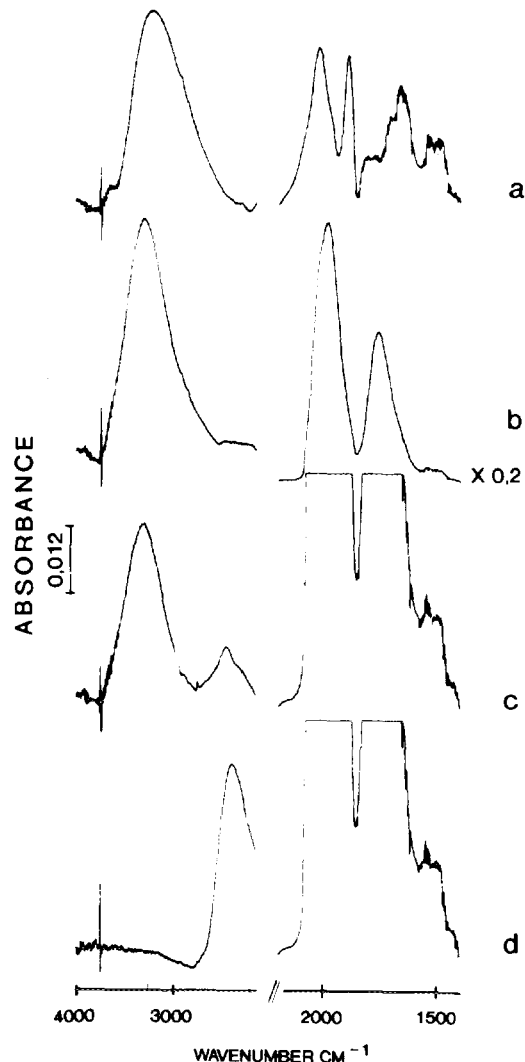


FIG. 3. (a) Infrared spectrum of hydrogen adsorbed on 2 wt% Pt-silicalite-Gas phase removed ($p = 10^{-1}\text{ Pa}$) for 5 min. (b) As for 3a but after having adsorbed CO ($p_{CO} = 0.5\text{ kPa}$). (c) and (d) As for (b) but having removed CO ($p = 10^{-1}\text{ Pa}$, 15 min, and adsorbed D_2 ($p = 0.5\text{ kPa}$). Spectra (c), (d) registered as a function of time: (c) 15 min, (d) 15 h.

Hence, the two IR vibrations at 3200 and 2030 cm^{-1} are only observed for Pt-silicalite.

(2) Formation of Adsorbed H_2 , Displacement with CO, and Exchange with Deuterium

In order to determine the stability of these hydrogen species, displacement of hydrogen with carbon monoxide has been studied: for this purpose, 2 wt% Pt-silicalite having chemisorbed H_2 was evacuated at RT for 5 min ($p = 10^{-1}\text{ Pa}$) (Fig. 3a): it appears that the vibration at 3200 cm^{-1} is unchanged, but by contrast, that at 2030 cm^{-1} is strongly reduced. Then the sample was contacted with CO ($p = 0.5\text{ kPa}$) and the spectrum registered (Fig.

3b): two well-known vibrations due to Pt–CO linear singleton (2060 cm^{-1}) and bridged CO species (1800 cm^{-1}) appeared (8). The broad band at 3200 cm^{-1} is slightly decreased and shifted to 3300 cm^{-1} ; it is not possible to know if the weak band at 2030 cm^{-1} due to hydrogen species is still existing because Pt–CO singleton vibration which is intense would overlap with it (if it is still existing).

Having removed CO gas phase ($p = 0.1\text{ Pa}$, 15 min), D_2 ($p = 0.5\text{ kPa}$) was introduced in the infrared cell, and the spectra were registered as a function of time.

Figure 3 indicates that H–D exchange is still operating but with a much lower rate than in absence of CO indicating that part of the sites on which H–D exchange is occurring are poisoned by CO; nevertheless, after 15 h, more than 90% of adsorbed hydrogen species have been exchanged with deuterium; a careful examination of Fig. 3 in the $1400\text{--}1600\text{ cm}^{-1}$ range does not indicate any IR vibration: this has to be compared with Fig. 2b in which the vibration of the deuterium species is observed at 1479 cm^{-1} . This result indicates that the two sets of hydrogen species vibrating at 3200 and 2030 cm^{-1} have not the same behaviour in presence of CO. The broad band at 3200 cm^{-1} is not deeply affected with the addition of CO (a decrease of 30% in absorbance is observed) and is still exchangeable with deuterium.

In order to know the behaviour, in presence of CO, of the species vibrating at 2030 cm^{-1} , a freshly reduced sample has been first contacted with deuterium giving the vibrations at 2393 and 1479 cm^{-1} ; then CO was added ($p = 0.5\text{ kPa}$). The species vibrating at 1479 cm^{-1} vanished indicating their displacement by CO. Thus, it is concluded that in presence of CO, only the hydrogen species vibrating at 3200 cm^{-1} are existing and exchangeable with deuterium. Additional IR experiments were performed such that the experimental conditions were identical to those used for volumetric measurements (see Table 1, last line):

—saturation with CO of a freshly reduced and evacuated 2 wt% Pt–silicalite,

— H_2 adsorption and then registration of the IR spectrum:

- the vibrations at 2060 (CO singleton) and 1800 cm^{-1} (bridged CO) are observed together with the vibration due to hydrogen species at 3300 cm^{-1} . The absorbance of this vibration is smaller than that observed on a freshly reduced surface nonsaturated with CO (30% less), and it will be labelled as A_{HCO} .

(3) Reaction of Preadsorbed Hydrogen Species with Oxygen (or Preadsorbed O_2 with H_2)

On the 2 wt% Pt–silicalite having preadsorbed H_2 (Fig. 4a), O_2 was introduced (0.5 kPa) at room temperature after having removed H_2 gas phase (5 min, $p = 0.1\text{ Pa}$). The

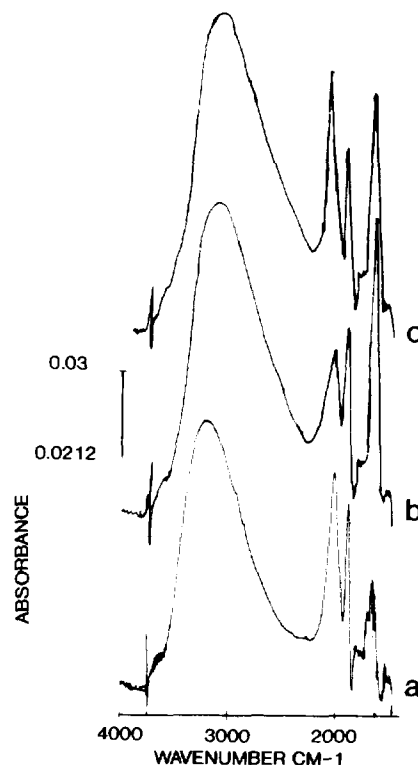


FIG. 4. Infrared spectra of hydrogen species on 2 wt% Pt–silicalite. (a) H_2 being adsorbed as in figure 2a and evacuated. (b) O_2 (0.5 kPa) was contacted the sample. (c) First O_2 adsorption (0.5 kPa) and evacuation (15 min, $p = 0.1\text{ Pa}$) then H_2 (0.5 kPa) adsorption.

spectrum (Fig. 4b) indicates that two IR bands appeared: a strong broad one $3600\text{--}3000\text{ cm}^{-1}$ with a maximum at 3000 cm^{-1} and a weaker sharp one at 1630 cm^{-1} . These vibrations are due to the formation of water (3600 cm^{-1} and 1630 cm^{-1}) and the previous hydrogen species vibrating at 3200 cm^{-1} . Because of the overlapping of the IR bands due to water and hydrogen species, it is not possible to conclude about the complete disappearance of the species at 3200 cm^{-1} .

The spectrum of figure 4b is qualitatively identical to that obtained (not reported here) on 2 wt% Pt silicalite having adsorbed water ($p = 0.1\text{ kPa}$) which exhibits a very broad peak ($3600\text{--}3000\text{ cm}^{-1}$) centered at 3300 cm^{-1} and a sharp peak at 1630 cm^{-1} . The reverse reaction, first O_2 adsorption on the bare surface and evacuation followed by H_2 adsorption has also been studied: the IR spectrum obtained (Fig. 4c) clearly indicated the presence of a broad band at 3200 cm^{-1} and 1630 cm^{-1} together with a weak vibration at 2030 cm^{-1} ; this result indicated that oxygen has reacted with hydrogen to form H_2O (vibrations at 1630 and 3000 cm^{-1}) and that previous hydrogen species characterized by IR bands at 3200 and 2030 cm^{-1} have been formed on Pt sites.

Finally, in Fig. 5, the change in absorbance of the IR vibration at 3200 cm^{-1} is reported as a function of Pt

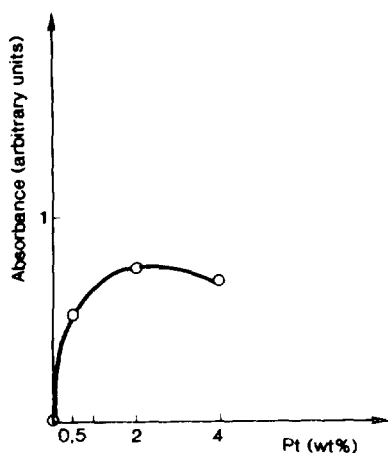


FIG. 5. Change in the absorbance of 3200 cm^{-1} vibration as a function of Pt loading.

loading: it is observed that the concentration in hydrogen species vibrating at 3200 cm^{-1} are not deeply changed when Pt loading is increased up to 4 wt% Pt.

Our results clearly show that the vibration at 3200 cm^{-1} is much more stable (under vacuum or in presence of CO) than that at 2030 cm^{-1} and is related with the very unusual high dispersion of platinum.

So, two important questions remain to be discussed:

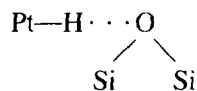
—What is the nature and the location of the hydrogen species vibrating at 3200 cm^{-1} ?

—Are these hydrogen species related to the extra hydrogen measured by volumetric measurements? (Assuming a stoichiometry $\text{H}/\text{Pt}_s = 1$, the excess of hydrogen adsorbed relative to this stoichiometry is called extra hydrogen).

Nature and location of hydrogen species vibrating at 3200 cm^{-1}

These hydrogen species are stable in presence of CO and their exchange (in presence and absence of CO) with D_2 suggests that these species are located either on Pt particles or in their surrounding.

Studying H-MFI zeolites by diffuse reflectance IR spectroscopy, Kazansky and co-workers (9) observed a broad vibration at 3200 cm^{-1} which was attributed to an OH group having an hydrogen bond with one of the neighbouring oxygen atoms of the zeolite framework. From the IR wavenumber value measured here, it can be proposed that the species under study could be due to hydrogen bonded to a Pt atom and interacting with a silicalite framework oxygen:



Recently (6, 10), it has been shown for Pt-KL that at least 3 different hydrogen species were existing after H_2 treatment at 300°C : from EXAFS, the authors have concluded that Pt-O distance (here O belonging to L zeolite framework) was modified in the presence of so called "interfacial hydrogen." This interfacial hydrogen located between the platinum particle and the zeolite support is desorbed at $300\text{--}400^\circ\text{C}$. This model reinforces our conclusion.

Since the hydrogen species are formed upon H_2 adsorption at RT, it is tempting to relate the presence of these hydrogen species to the extra hydrogen. In Table 1 it is indicated that the Pt-silicalite saturated with CO and evacuated at RT adsorbed a relatively small amount of H_2 ($\text{H}/\text{Pt} = 0.08$) (Table 1).

In the same experimental conditions, the IR vibration (3300 cm^{-1}) due to hydrogen species is formed with an absorbance labelled A_{HCO} .

Thus, it could be suggested that the quantity of hydrogen chemisorbed $0.08\text{ H}/\text{Pt}$ ($4.4\text{ }\mu\text{mol H}_2/\text{g solid}$) corresponds to the formation of hydrogen species vibrating at 3300 cm^{-1} and having a total absorbance 30% smaller than that obtained on the sample not saturated with CO; Table 1 indicates that for 2 wt% Pt-silicalite total hydrogen adsorption is $63.8\text{ }\mu\text{mol H}_2/\text{g}$ (IR absorbance labelled A_{H}). A $\text{H}/\text{Pt} = 1$ would consume $63.8/1.25 = 51\text{ }\mu\text{mol H}_2/\text{g solid}$; so the extra hydrogen adsorption can be evaluated to $12.8\text{ }\mu\text{mol H}_2/\text{g solid}$ and if the previous assumption is true should correspond to an IR vibration having A_{H} absorbance with: $A_{\text{H}} = 12.8/4.4 A_{\text{HCO}} = 2.9 A_{\text{HCO}}$.

Experiments give $A_{\text{H}}/A_{\text{HCO}} = 1.3$. So there is apparently no quantitative relation between IR measurements and volumetric data.

To explain this, it has been assumed that the extinction coefficients of hydrogen species were the same, in presence or in absence of CO. Since it is observed that presence of CO the hydrogen species are vibrating at 3300 cm^{-1} compared to 3200 cm^{-1} in absence of CO, this change could also be reflected in a change in the extinction coefficient, this rendering difficult the quantification of IR results. Finally, Fig. 5 in which the absorbance of these hydrogen species is plotted as a function of Pt loading indicates that the relative contribution of these hydrogen species to the total amount of chemisorbed hydrogen (as measured by volumetry) is decreasing with the Pt loading (see also Table 1). So, it is mainly for low Pt loadings (<2 wt% Pt) that this extra hydrogen is clearly evidenced.

Nature and location of hydrogen species vibrating at 2030 cm^{-1} . Since these species are not stable under vacuum they are not related with the extra hydrogen previously considered. It is known from the literature that metal-hydrogen stretching band are formed during adsorption of H_2 over metals like Ir (11), Rh (12, 13), or Pt

(14, 15). Due to the low hydrogen pressure used here, the 2120 cm^{-1} vibration formed on Pt/ Al_2O_3 (14) or Pt/ SiO_2 (15) for high hydrogen pressures was not observed here.

Recently, Wey et al. (12) have shown that the existence of Rh-H species is pressure dependent since at low H_2 pressures, no IR vibration is observed. The behaviour of hydrogen species observed here suggests that they could be hydride species. The reason of their formation on Pt-silicalite could be related to the presence of very small Pt particles, but no explanation is proposed for their formation.

CONCLUSIONS

Deposition of Pt on silicalite support gives highly dispersed Pt particles exhibiting peculiar behaviour towards hydrogen chemisorption.

Volumetric measurements indicate that for the highly dispersed Pt particles, H/Pt values larger than one are obtained. Infrared studies suggest that the extra hydrogen measured could be related to hydrogen species bonded to Pt and to framework oxygen.

ACKNOWLEDGMENT

Indo-French Center for the promotion of Advanced Research (IFCPAR) New Delhi is acknowledged for its funding.

REFERENCES

1. Sachtler, W. M. H. and Zhang, Z., "Advances in Catalysis," Vol. 39, p. 129. Academic Press, London, 1993.
2. Dalla Betta, R. A. and Boudart, M., "Proceedings, 5th Int. Cong. on Catal., Palm Beach, 1972" (J. W. Hightower Ed) p. 132. North Holland, Amsterdam, 1973.
3. Dimitriev, R. V., Detjuk, A. N., Minachev, Kh., and Steinberg, K. "Spillover of adsorbed species," in *Studies Surface Science and Catalysis*, Vol. 17, p. 17. Elsevier, Amsterdam, 1983 and references therein.
4. Lin, S. D., and Vannice, M. A. *J. Catal.* **143**, 539 (1993).
5. Mériaudeau, P., Thangaraj, A., Narayanan, S., and Naccache, C., *J. Catal.* **146**, 579 (1994).
6. Koningsberger, D. C., and Gates, B. C., *Catal. Lett.* **14**, 271 (1992).
7. Gallezot, P., *Catal. Rev. Sci. Eng.* **20**, 121, (1979).
8. Blyholder, G. J., *J. Phys. Chem.* **79**, 756 (1975).
9. Zholobenko, V. L., Kustov, L. M., Borovkov, V. Y., and Kazansky, V. B., *Zeolites* **8**, 175 (1988).
10. Miller, J. T., Meyers, B. L., Modica, F. S., Lane, G. S., Vaarkamp, M., and Koningsberger, D. C., *J. Catal.* **143**, 395 (1993).
11. Bozon-Verduraz, F., Contour, J., Pannetier, G., *C.R. Acad. Sci. (Paris)* **269**, 1436 (1969).
12. Wey, J. P., Neely, W. C., and Worley, S. D., *J. Phys. Chem.* **95**, 8881 (1991).
13. Fang, T. H., Wey, J. P., Neely, W. C., and Worley, S. D., *J. Phys. Chem.* **97**, 5128 (1993).
14. Primet, M., Basset, J. M. and Mathieu, M. V., *J. Chem. Soc. Faraday Trans. 1* **70**, 293 (1974).
15. Szilagyi, T., *J. Catal.* **121**, 223 (1990) and references therein.

Preparation, Structural Properties, and Hydrogenation Activity of Highly Porous Palladium–Titania Aerogels

M. Schneider, M. Wildberger, M. Maciejewski, D. G. Duff, T. Mallát, and A. Baiker¹

Department of Chemical Engineering and Industrial Chemistry, Swiss Federal Institute of Technology, ETH-Zentrum, 8092 Zürich, Switzerland

Received December 17, 1993; revised March 4, 1994

Mesoporous to macroporous palladium–titania aerogels with high surface area have been synthesized by the sol–gel–aerogel route. A titania gel was prepared by the addition of an acidic hydrolysant to tetrabutoxytitanium(IV) in methanol. The palladium precursor solutions, added after the redispersion of the titania gel, were either Na_2PdCl_4 , $(\text{NH}_4)_2\text{PdCl}_4$, $\text{Pd}(\text{acac})_2$, or $\text{Pd}(\text{OAc})_2$ dissolved in protic or aprotic solvents. The palladium–titania aerogels have a BET surface area of $170\text{--}190\text{ m}^2\text{ g}^{-1}$ after a thermal treatment up to 673 K and contain well-developed anatase crystallites of about 7–8 nm mean size. Depending on the palladium precursor used, the volume-weighted-mean particle size, determined by TEM, varies significantly in the range 21–224 nm, this being independently consistent with XRD line-broadening results. All aerogel samples showed pronounced structural stability of both the titania matrix and the palladium particles towards the pretreatment media used (air or hydrogen) at temperatures up to 773 K. Thermal analysis, combined with mass spectrometry, revealed that the untreated catalysts contain a considerable amount of entrapped organic impurities after high-temperature supercritical drying. Liquid-phase hydrogenations of *trans*-stilbene and benzophenone were used as test reactions for characterizing the activity and accessibility of the palladium particles. A comparison of the best dispersed $\text{Pd}(\text{OAc})_2$ -derived aerogel catalysts with conventionally impregnated titania-supported palladium catalysts in the liquid-phase hydrogenation of 4-methylbenzaldehyde reveals superior activity and selectivity for the aerogel catalysts. © 1994 Academic Press, Inc.

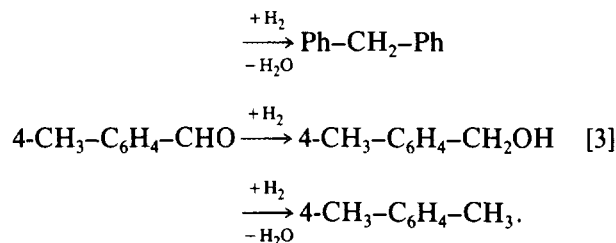
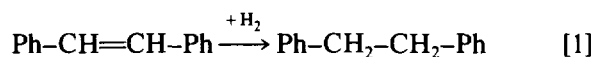
INTRODUCTION

The potential of aerogels for catalysis resides in their unique morphological and chemical properties (1–3). These originate from their wet chemical preparation by the solution–sol–gel (SSG) method (4) and the subsequent removal of solvent via supercritical drying (SCD). Due to the “structure-preserving” ability of SCD (5), the aerogels are usually solids of high porosity and specific surface area. Mixed gels of *in situ* reduced Group VIII metals, highly dispersed and uniformly distributed in different

metal oxide matrices are readily synthesized by this combination of the SSG-technology with ensuing SCD (6–8).

Based on our previously published method for synthesis of meso- to macroporous titania aerogels with high surface area (9), we recently demonstrated the direct preparation of highly dispersed Pt–titania aerogels possessing marked structural stability and excellent hydrogenation activity (6). This and the increasing academic as well as commercial interest in titania-supported Group VIII metal catalysts (especially for carbonyl-group hydrogenation) (10–12) prompted us to extend our studies to palladium–titania aerogel catalysts.

Applying the same method for the wet chemical SSG-process as in Ref. (6), consisting of preformation of the titania gels and their subsequent redispersion followed by the addition of different Pd precursor solutions before SCD, we aimed to prepare stable, mesoporous palladium–titania aerogels with high specific surface areas. For testing the accessibility and activity of the palladium particles, the liquid-phase hydrogenations of *trans*-stilbene (Eq. [1]), benzophenone (Eq. [2]), and 4-methylbenzaldehyde (Eq. [3]) were chosen:



trans-Stilbene, benzophenone, and 4-methylbenzaldehyde are all bulky molecules favoured by catalysts with wide pores and they possess different functional groups

¹ To whom correspondence should be addressed.

(C=C double bond or carbonyl group). In addition to the low-temperature liquid-phase hydrogenation, which is especially suitable for bulky molecules, we also investigated the effects of different pretreatment procedures on the structural and catalytic properties.

EXPERIMENTAL

Sol-Gel-Aerogel Synthesis

Throughout the text the following scheme of abbreviations is used, taking Pd5PAC as an example. The numeral following "Pd" designates the Pd content in wt% and the subsequent letters represent the Pd precursor used ($\text{Na}_2\text{PdCl}_4 \rightarrow \text{PC}$; $(\text{NH}_4)_2\text{PdCl}_4 \rightarrow \text{NP}$; $\text{Pd}(\text{acac})_2 \rightarrow \text{PA}$; $\text{Pd}(\text{OAc})_2 \rightarrow \text{PAC}$). These acronyms describe the original (untreated) aerogel materials.

Analytical grade reagents were used throughout this work. The preparation of the palladium-titania aerogels is derived from that for Pt-titania reported in Ref. (6), and consequently only a short description will be given here. The SSG process was carried out in an anti-adhesive, closed Teflon beaker, under nitrogen atmosphere and at ambient temperature (297 ± 2 K). First, the acidic hydrolysant diluted with methanol was added to a methanolic solution of tetrabutoxytitanium(IV). The resulting titania gels were aged for 4 h and then redispersed with different amounts of methanol (Table 1). The Pd precursor solution (Table 1) was added to the nonviscous titania solution and a second ageing step for 19 h under vigorous stirring followed (ca. 1000 rpm). With Pd2PC and Pd2NP, red-orange translucent solutions developed, while in the case of Pd2PA the solution was yellow and translucent. With Pd2PAC and Pd5PAC, the initially red-orange colour turned to dark green and then black within minutes. These solutions were highly viscous in the case of Pd2PC and Pd2NP.

The as-prepared sol-gel product was transferred in a Pyrex-glass liner into an autoclave with a net volume of 1.09 l together with the appropriate amount of additional

methanol (outside of the liner) (Table 1), thus exceeding the critical volume of the mixed solvent (solvent volume ca. 375 ml in all cases). The corresponding critical data for methanol, as the dominating component of all five SSG-solvents, are $V_c = 118$ ml mol⁻¹, $T_c = 513$ K, and $p_c = 8.1$ MPa (13). The SCD conditions were set as follows (6): nitrogen prepressure of 5 MPa, heating rate of 1 K min⁻¹ to final SCD temperature of 533 K, 30 min thermal equilibration (final pressure about 19 MPa) and isothermal depressurization with 0.1 MPa min⁻¹. As represented in Table 1, the precursor solution of Pt2PA contained 30 ml of benzene ($T_c = 562$ K (14)), which was compensated for by a 5 K increase of the SCD end-temperature. The resulting grey aerogel clumps were then ground in a mortar.

Finally, portions of the untreated (raw) aerogel powders were thermally treated in a tubular reactor with upward flow. The media applied were air, air followed by hydrogen or hydrogen. The pretreatment temperatures ranged from 473 to 773 K. Detailed descriptions of the single pretreatment processes are given in Ref. (6). The only exceptions are the thermal treatments of two Pd2PA samples calcined in the same way as the standard air treatment, but at temperatures of 723 and 773 K, respectively. Moreover, portions of Pd2PA, Pd2PAC, and Pd5PAC were heated in air at 1 K min⁻¹ and kept at 373 K for 8 h. Then the temperature was increased to 473 K at 0.5 K min⁻¹ and held for 11 h.

The metal loading was generally calculated on the basis of the nominal amounts used (Table 1) and the assumption of a complete reduction of the Pd precursors. The nominal metal loadings were independently confirmed by oxidation-decomposition analysis. The assumption of the complete reduction is justified on the basis of published data (15) concerning the preparation of Pd sols in refluxing methanol (338 K and ambient pressure). Note that we used 533 K and a methanolic pressure of ca. 10 MPa.

Nitrogen Physisorption

The specific surface areas (S_{BET}), mean cylindrical pore diameters ($\langle d_p \rangle$) and specific adsorption pore volumes

TABLE 1
Compositions of the Palladium Precursor Solutions, Amount of Methanol (MeOH) Used for the Redispersion of the Titania Gels and Extra Amount of MeOH Added for the Supercritical Drying

Aerogel	Precursor (mg)	Solvent composition (ml)	MeOH for redispersion (ml)	Extra MeOH for SCD (ml)
Pd2PC	PdCl ₂ (256) NaCl (168)	H ₂ O (1.0)/ MeOH (24)	71	130
Pd2NP	(NH ₄) ₂ PdCl ₄ (410)	H ₂ O (2)/MeOH (24)	71	130
Pd2PA	Pd(acac) ₂ (440)	Benzene (30)	71	124
Pd2PAC	Pd(OAc) ₂ (324)	Acetone (24) (warm)	71	130
Pd5PAC	Pd(OAc) ₂ (835)	Acetone (40) (warm)	55	130

(V_{PN_2}) were derived from nitrogen physisorption measurements at 77 K using a Micromeritics ASAP 2000 instrument. Prior to measurement, all samples were degassed to 0.1 Pa at 423 K. BET surface areas were calculated in a relative pressure range of 0.05 to 0.2 assuming a cross-sectional area of 0.162 nm² for the nitrogen molecule. The pore size distributions were calculated applying the Barrett–Joyner–Halenda (BJH) method (16) to the desorption branches of the isotherms (17). The assessments of microporosity were made from t -plot constructions ($0.3 < t < 0.5$ nm), using the Harkins–Jura correlation (18).

X-Ray Diffraction

X-ray powder diffraction (XRD) patterns were measured on a Siemens Θ/Θ D5000 powder X-ray diffractometer. The diffractograms were recorded with detector-sided Ni-filtered $K\alpha\text{Cu}$ radiation over a 2Θ -range of 20° to 90° and a position-sensitive detector. The mean crystallite sizes were determined using the Scherrer equation (19) and the (101)- or (200)-reflection for anatase (20), the (111)-reflection for Pd (21), and the (110)-reflection for PdO (22).

Transmission Electron Microscopy

Samples for transmission electron microscopy (TEM) were loaded dry onto perforated, thin carbon films supported on copper grids, aerogel powder being poured five times onto the carbon film and shaken off.

Diffraction-contrast TEM was performed using a Hitachi H-600 electron microscope operated at 100 kV, with a point resolution of ca. 0.5 nm. The instrumental magnification had previously been calibrated using the phase contrast from catalase crystals. Identification of the palladium component used its usually greater contrast in comparison to the less electron-dense titania, as well as the different particle morphologies. However, where the palladium size data overlapped with the size range of the anatase primary crystallites (5–11 nm), identification was hardly possible due to the rather limited and orientation-dependent contrast differences. The evaluation and representation of the measured particle size distribution is described in more detail in Ref. (6).

Briefly, the most important parameters obtained from the distribution data were the mean diameter from the volume-weighted ($\langle d \rangle_v$) and the mean diameter from the (surface-)area-weighted distribution ($\langle d \rangle_a$). The number of palladium particles measured varied from 25 to 44. The breadth of the size distributions was expressed by the coefficient of variation, the root-mean-square (standard) deviation of diameters from the (unweighted) mean expressed as a (percent) fraction of this mean.

Thermal Analysis

TG and DTA investigations were performed on a Netzsch STA 409 instrument coupled with a Balzers QMG

420/QMA 125 quadrupole mass spectrometer, equipped with Pt–Rh thermocouples and Pt crucibles. A heating rate of 10 K min⁻¹ and an air flow of 25 ml min⁻¹ were used. The sample weight was ca. 32 mg and the $\alpha\text{-Al}_2\text{O}_3$ reference weight 62.5 mg.

Total carbon and hydrogen contents were determined with a LECO CHN-900 elemental microanalysis apparatus.

Catalytic Characterization

Trans-stilbene and benzophenone hydrogenation were performed at 303 and 343 K, respectively, and at atmospheric hydrogen pressure. Isopropylacetate (*trans*-stilbene) and butylacetate (benzophenone) were used as solvents. The semibatch apparatus and experimental procedure, as well as the analysis of the product mixtures were described in detail in a previous report (6).

To minimize the influence of side reactions, the initial rates were determined from reactant consumption at below 5% conversion. Preliminary tests with the most active aerogel catalyst, in which the amount of catalyst, stirring speed and granule fraction were varied within a wide range showed that the reaction rate in [mol s⁻¹ (g_{Pd})⁻¹] was independent of the amount of catalyst (≤ 50 mg), the stirring speed (≥ 500 rpm) as well as the particle size (≤ 500 μm), indicating that interparticle and intraparticle mass transfer control could be ruled out. For a few of the most active catalysts the experimental errors of the catalytic testing were determined, estimated from three consecutive measurements. They ranged between 5 and 10%.

The hydrogenation of 4-methylbenzaldehyde was performed in the same semi batch apparatus as mentioned above. A 1 wt% ethanolic solution of 4-methylbenzaldehyde was hydrogenated with 10–30 mg aerogel powder (< 300 μm) at 35 ml min⁻¹ hydrogen flow (atmospheric pressure) and 333 ± 1 K. The Pd:reactant weight ratio was kept constant at 1:40. Samples of the reaction mixture (ca. 0.3 ml) were periodically taken, filtered, and analyzed using gas chromatography (6).

RESULTS

Properties of the palladium-titania aerogels are listed in Table 2.

Nitrogen Physisorption

Figure 1 depicts as a representative example the adsorption/desorption isotherms and differential pore size distribution of the Pd5Pac sample, calcined in air at 573 K. All aerogel samples showed a type-IV isotherm with a type-H1 desorption hysteresis according to IUPAC-classification (23). They all possess pronounced meso- to macroporosity and only little microporosity, yielding pore-